Title
Dynamic changes of substrate reactivity and enzyme adsorption on partially hydrolyzed cellulose

Journal
Biotechnology and Bioengineering, 114(3)

ISSN
00063592

Authors
Shi, Jian
Wu, Dong
Zhang, Libing
et al.

Publication Date
2016-11-28

DOI
10.1002/bit.26180

Peer reviewed

ARTICLE

BIOTECHNOLOGY and BIOENGINEERING

Dynamic Changes of Substrate Reactivity and Enzyme Adsorption on Partially Hydrolyzed Cellulose

Jian Shi,[1,2,3] Dong Wu,[2,4] Libing Zhang,[5] Blake A. Simmons,[2] Seema Singh,[2,4] Bin Yang,[1,5] Charles E. Wyman[1,6,7]

[1]Center for Environmental Research and Technology, University of California, 1084 Columbia Avenue, Riverside, CA 92507; telephone: 951-827-6238; fax: 951-827-5696; e-mail: cewyman@engr.ucr.edu

[2]Deconstruction Division, Joint BioEnergy Institute, Emeryville, California

[3]Department of Biosystems and Agricultural Engineering, University of Kentucky, Lexington, Kentucky

[4]Biological and Materials Science Center, Sandia National Laboratories, Livermore, California

[5]Bioproducts, Sciences and Engineering Laboratory, Department of Biological Systems Engineering, Washington State University, Richland, Washington

[6]Department of Chemical and Environmental Engineering, Bourns College of Engineering, Riverside, California

[7]BioEnergy Science Center, Oak Ridge National Laboratory, Oak Ridge, Tennessee

ABSTRACT: The enzymatic hydrolysis of cellulose is a thermodynamically challenging catalytic process that is influenced by both substrate-related and enzyme-related factors. In this study, a proteolysis approach was applied to recover and clean the partially converted cellulose at the different stages of enzymatic hydrolysis to monitor the hydrolysis rate as a function of substrate reactivity/accessibility and investigate surface characteristics of the partially converted cellulose. Enzyme-substrate interactions between individual key cellulase components from wild-type *Trichoderma reesei* and partially converted cellulose were followed and correlated to the enzyme adsorption capacity and dynamic sugar release. Results suggest that cellobiohydrolase CBH1 (Cel7A) and endoglucanases EG2 (Cel5A) adsorption capacities decreased as cellulose was progressively hydrolyzed, likely due to the "depletion" of binding sites. Furthermore, the degree of synergism between CBH1 and EG2 varied depending on the enzyme loading and the substrates. The results provide a better understanding of the relationship between dynamic change of substrate features and the functionality of various cellulase components during enzymatic hydrolysis.

Biotechnol. Bioeng. 2017;114: 503–515.

KEYWORDS: cellulose; proteolysis; reactivity; cellulase; enzyme–substrate interactions

Correspondence to: Dr. C.E. Wyman
Contract grant sponsor: Ford Motor Company and Mascoma Corporation
Contract grant sponsor: Office of Science, Office of Biological and Environmental Research, of the U.S. Department of Energy
Contract grant number: DE-AC02-05CH11231
Contract grant sponsor: DARPA Young Faculty Award
Contract grant number: N66001-11-1-414
Contract grant sponsor: National Science Foundation
Contract grant number: 1355438
Received 15 June 2016; Revision received 29 August 2016; Accepted 5 September 2016
Accepted manuscript online 5 September 2016;
Article first published online 28 November 2016 in Wiley Online Library (http://onlinelibrary.wiley.com/doi/10.1002/bit.26180/abstract).
DOI 10.1002/bit.26180

Introduction

The most expensive operations in biological processing of cellulosic biomass to fuels and chemicals are needed to release sugars with high yields from this naturally recalcitrant material. Unfortunately, such bioprocessing technologies struggle for commercial viability, at least partly because high enzyme doses are currently required to hydrolyze cellulose to glucose at the high yields vital to economic success (Wooley et al., 1999) and to compensate for the rapid fall-off in hydrolysis rate as conversion progresses (Desai and Converse, 1997; Eriksson et al., 2002; Ragauskas et al., 2006). For example, the typical cellulase loadings of about 15 FPU/g cellulose used to achieve high yields of sugars from pretreated biomass could be translated into about 30 g of enzyme per liter of ethanol made, an extremely high and expensive dose. Thus, enzyme costs must either be reduced below about $2/kg protein or strategies developed to

substantially reduce loadings (Himmel et al., 1999; Wingren et al., 2005; Wyman, 2007; Yang et al., 2011). The limited understanding of hydrolysis reaction mechanisms and factors controlling hydrolysis effectiveness impede many promising applications in the real world (Himmel et al., 2007; Igarashi et al., 2011). In particular, the rapid decline in cellulose hydrolysis rates over reaction time contributes to high enzyme demands, but the mechanism responsible for the resulting high cost of biomass bioconversion is not well understood. Previous results showing that the reactivity of pure cellulose (Avicel, microcrystalline cellulose) did not change appreciably with conversion by commercial cellulases (Yang et al., 2006) indicated that the drop off in reaction rate for continual cellulose digestion could not be attributed to changes in the substrate reactivity and pointed to other effects such as enzymes getting "stuck" or "jamming," slowing down, and effects of cellulose intermediates being responsible (Igarashi et al., 2011; Sugimoto et al., 2012).

Researchers have proposed a number of hypotheses to explain this observation that can be generally be viewed in terms of two groups: substrate related factors and enzyme related factors (Yang et al., 2011). Enzyme related factors may include thermal denaturation/deactivation of cellulases, inhibition by hydrolysis intermediates, enzyme slowing down/stopping, improper enzyme loading and activity combinations, and competition or enzyme crowding on the cellulose surface. Substrate related factors that can greatly affect hydrolysis rates include changes in crystallinity and DP, alternation/reduction of binding sites, heterogeneous structure of the substrate, and transformation into a less digestible form (Mansfield et al., 1999).

Further complicating the investigation is that enzyme synergism, commonly observed among cellulases, is influenced by both enzyme sources and substrate features (Van Dyk and Pletschke, 2012). Based on widely accepted "exo-endo" synergy, endoglucanases hydrolyze internal glycosidic bonds of cellulose chains after which cellobiohydrolase act as exoglucanases and split off cellobiose units from the reducing or non-reducing chain ends. This "exo-endo" synergism is based on the assumption that the two types of cellulases attack different regions of the cellulose chain and create new binding/attacking sites for each other. However, substrate properties, especially cellulose heterogeneity and physical characteristics, and enzyme properties, such as enzyme types, ratios of different enzyme activities, and enzyme-to-substrate ratios, all affect the synergism among enzymes during cellulose hydrolysis.

Although previous research provided valuable insights into cellulose–cellulase interactions during hydrolysis, only very few monitored enzyme activity on cellulose with a "clean surface." By removing reacted enzymes from partially hydrolyzed cellulose and adding fresh enzymes back to the remaining cellulose, this "restart" protocol delineared factors associated with cellulase alterations (Yang et al., 2006). As a result, property and structure changes of cellulose and the influence on enzymes during enzymatic hydrolysis can be investigated. Furthermore, the full understanding of the cooperative action of cellulases requires observation of both synergistic sugar production and enzyme adsorption in the same experiments, since it is the adsorbed enzyme that causes hydrolysis.

To better understand the mechanism of enzymatic hydrolysis of cellulose, the study reported here applied a restart protocol (Yang et al., 2006) to measure how cellulose reactivity changed and the interaction of cellulose with key cellulase components over the course of enzymatic hydrolysis. This approach allowed us to accurately monitor the hydrolysis rate as a function of substrate reactivity/accessibility and surface characteristics of partially converted cellulose while excluding the impact of cellulase changes over the hydrolysis period. Accordingly, purified cellobiohydrolase CBH1 (Cel7A) and endoglucanases EG2 (Cel5A) from wild-type *Trichoderma reesei* were used to investigate the effect of enzyme-substrate interactions on reaction rates. Synergism of these key components was studied to investigate their cooperativity on partially hydrolyzed cellulose.

Materials and Methods

Materials

Avicel PH101 (Lot No. 1344705) is a microcrystalline cellulose (MCC) containing more than 97% cellulose and less than 0.16% water soluble materials. Cellulose hydrolysis was performed using the complete *T. reesei* cellulase system Spezyme CP with protein content of 116 mg/mL and cellulase activity of 62 FPU/mL (DuPont Industrial Biosciences (formerly Genencor, a Danisco Division), Palo Alto, CA) and a commercial β-glucosidase preparation Novozyme 188 with a protein content of 125 mg/mL and activity of ~665 CBU/mL (Sigma–Aldrich, St. Louis, MO). Purified CBH 1 (Cel7A by CAZy nomenclature, Lot# 080703) and EG2 (Cel5A by CAZy nomenclature, Lot# 061207) derived from wild-type *T. reesei* with >98% purity (determined using SDS–PAGE) were generously provided by DuPont Industrial Biosciences (formerly Genencor, a Danisco Division). The purified CBH1 and EG2 fractions were concentrated by ultrafiltration to >30 mg protein/mL using Vivaspin 15R concentrators (Viva-products, Littleton, MA) with 10 kDa MW cut-off against 50 mM sodium acetate buffer (pH 4.8). The amount of enzymes was translated from mass to moles or vice versa based on the following molecular weights: CBH1, 64,000 g/mol and EG2, 48,000 g/mol (Ståhlberg et al., 1991).

Preparation of Partially Hydrolyzed Cellulose

Enzymatic hydrolysis of Avicel was interrupted at 1, 2, 4, 5, 15 h at an enzyme loading of 60 FPU Spezyme CP plus 120 CBU of Novozyme 188 per gram cellulose. The solids and liquid were separated by centrifugation. Avicel and the solid residues were washed using the proteolysis approach described previously (Yang et al., 2006). The washed solids were lyophilized (Labconco, Kansas City, MO) and weighed. The partially hydrolyzed cellulose samples had experienced 0%, 28%, 41%, 68%, 74%, and 81% conversion of glucan (Table I).

Physiochemical Characterization of Partially Hydrolyzed Cellulose

Crystallinity index (CrI) of the partially hydrolyzed cellulose was measured by an X-ray diffractometer. CrI was calculated from the height ratio between the intensity of the crystalline peak (I_{002}-I_{AM})

Table I. Properties of raw and partially hydrolyzed micro-crystalline cellulose (MCC, brand name: Avicel).

Stop time, h	0	1	2	4	5	15
Conversion, %	0.0 ± 0.0	28.4 ± 0.2	40.8 ± 1.8	68.1 ± 0.8	74.3 ± 6.5	80.8 ± 1.3
Reducing ends[a]	24.6 ± 2.2	26.5 ± 2.7	28.5 ± 1.7	26.8 ± 0.5	27.8 ± 3.2	21.8 ± 1.3
Reactivity[b], %	25.3 ± 1.0	26.2 ± 2.1	23.5 ± 0.6	24.1 ± 0.9	22.4 ± 1.0	21.9 ± 0.2
CrI, %	65.1 ± 0.9	69.7 ± 3.7	67.6 ± 1.8	72.8 ± 1.0	74.0 ± 0.7	72.1 ± 0.5

[a]Unit: 10^{-6} mol glucose equivalence per gram cellulose.
[b]In term of 1st hour hydrolysis rate, % of loaded cellulose.

and total intensity (I_{002}) after subtraction of the background signal measured without cellulose (Park et al., 2010).

Attenuated total reflection-Fourier transform infrared spectroscopy (ATR-FTIR) was conducted on a Bruker Optics Vertex system (Billerica, MA) with built-in diamond–germanium ATR single reflection crystal. Partially hydrolyzed cellulose samples were pressed uniformly against the diamond surface using a spring-loaded anvil. Sample spectra were obtained in duplicates using an average of 128 scans over the range from 850 to 2000 cm^{-1} with a spectral resolution of 2 cm^{-1}. Baseline correction was performed using the rubberband method as described elsewhere (Singh et al., 2009).

Raman spectra were collected using a Bruker MultiRAM FT-Raman spectrometer equipped with a 1064 nm diode laser (Bruker Optics, Inc., Billerica, MA). A laser power of 100 mW was applied to all samples to provide sufficient signal-to-noise (S/N) ratios without saturating the detector. A total of 128 scans were performed on each cellulose sample with the spectral resolution set at 4 cm^{-1}. The acquired spectra in the range of 200–3400 cm^{-1} were smoothed and baseline corrected using OPUS software (Bruker Optics, Inc., Billerica, MA). Raman peaks related to cellulose (Table SI) were assigned based on databases reported elsewhere (Larsen and Barsberg, 2010; Wiley and Atalla, 1987).

The surface morphology and ultra-structure of the freeze-dried cellulose particles were imaged by using an Asylum Research MFP-3D atomic force microscopy (AFM) system (Santa Barbara, CA). All cellulose samples are fixed on small metal plates. Because the samples were in powder form, all cellulose powders were spread homogenously on a metal plate that had been painted with a thin epoxy layer to fix the cellulose particles in a form suitable for the AFM system. Then, a freshly peeled mica thin layer was pressed against the cellulose powders to generate a smoother flat surface and the epoxy allowed to dry with a nitrogen gas spraying off the top covered mica. Due to the steep surface slope, a high aspect ratio cantilever (MSS_FMP-13 from NanoTools) was selected as the AFM probe. The scan size ranged from a couple of microns to a couple of hundred nanometers, with the highest resolution being <1 nm. All images were processed using Igor software (Asylum Research AFM systems).

CBH1 and EG2 Adsorption on Cellulose When Loaded Alone

Cellulase adsorption was conducted in 1.5 mL Eppendorf LoBind microcentrifuge tubes (protein loss $<3\%$, Catalog# Z666491, Sigma–Aldrich). An appropriate amount of concentrated CBH1 or EG2 was mixed with partially hydrolyzed cellulose samples in 50 mM pH 4.8 acetate buffer to achieve a final enzyme loading of $\sim$0–2.5 μmol protein per gram cellulose. The mixtures were incubated at 4°C for 4 h to equilibrate, and then the solids and liquid were separated by centrifugation at 8000 rcf for 1 min at 4°C. Protein concentrations in the liquid fraction (μmol/mL) were measured at a wave length of 280 nm (UV) by a SpectraMax M2 spectrometer (Molecular Devices, Sunnyvale, CA) and used to calculate protein binding to cellulose using the following extinction coefficients ($M^{-1}\,cm^{-1}$): 78,800 and 64,000 for CBH1 and EG2, respectively (Ståhlberg et al., 1991).

CBH1 and EG2 Adsorption on Cellulose When Loaded Together

For synergistic enzyme adsorption, CBH1 was labeled by a Alexa Fluor 594 (AF594) succinimidyl esters kit (Molecular Probes, Inc., Eugene, OR) prior to mixing with EG2. First, 50 μL of 1 M bicarbonate was mixed with 0.5 mL of CBH1 protein solution ($\sim$1 mg protein) and an appropriate amount of reactive dye. The reaction mixture was incubated with stirring at room temperature for 90 min. Labeled protein was separated from excess dye by running the reaction mixture through a size exclusion purification resin column. AF594-labeled CBH1 was collected in a 1.5 mL Eppendorf LoBind microcentrifuge tube and used immediately for adsorption. The AF594 label was functionalized with N-hydroxysuccinimidyl ester that reacts with the primary amines of lysine residues in the enzyme. Similarly, labeled cellulases have been shown previously to retain their original activity on cellulose (Jeoh et al., 2002).

AF594-labeled CBH1 together with equal molar unlabeled EG2 were added to interrupted Avicel samples in 50 mM pH 4.8 acetate buffer to achieve a final CBH1 and EG2 loading of $\sim$0–2.0 μmol protein for each enzyme per gram cellulose. Adsorption mixtures were incubated at 4°C for 4 h to equilibrate, and then the solids and liquid were separated by centrifugation. Total free protein concentrations in the liquid fraction (μmol/mL) were measured at a 280 nm UV wavelength by a SpectraMax spectrometer (Molecular Devices) (Ståhlberg et al., 1991). The concentrations of AF594 labeled CBH1 were determined by correlating the fluorescence intensity of the fluorophores with protein concentrations at suggested excitation/emission wavelengths for CBH1 of 594 and 617 nm, respectively. EG2 concentrations in the liquid (mg/mL) were extrapolated by subtracting CBH1 measured by fluorescence from total free protein in the liquid measured at 280 nm and used to calculate protein binding to cellulose.

Isothermal Adsorption Models

The Langmuir isotherm equation (Beldman et al., 1987) was used to describe cellulase adsorption on cellulose, with the parameters estimated by the non-linear optimization toolbox in MatLab 7.5 (The MathWorks, Inc., Natick, MA):

$$E_{\text{bound}} = \frac{\sigma \cdot E_{\text{free}}}{k_{\text{d}} + E_{\text{free}}} \quad (1)$$

In Equation (1), E_{bound}, E_{free}, σ, and k_{d} represent the amount of cellulase adsorbed on the solids (mg/g solids), the amount of cellulase remaining in solution (mg/mL), the maximum cellulase adsorption capacity (mg/g solids), and the equilibrium constant (mg/mL), respectively.

Hydrolysis of Partially Hydrolyzed Cellulose and Sugar Quantification

Partially hydrolyzed cellulose was hydrolyzed with individual cellulase components or their mixtures at different loadings at 50°C for 1 and 24 h, respectively. After hydrolysis, the liquid and solids were separated by centrifugation, and the residual solids were washed, dried, and weighed to estimate cellulose solubilization. Glucose and cello-oligomers in hydrolysate were measured using a Dionex IC equipped with electrochemical detector and CarboPac PA100 column and calibrated by sugar standards of glucose, cellobiose, and cellotriose (Sigma–Aldrich). DP>3 cellodextrins were estimated by subtracting glucose, cellobiose, and cellotriose from total cellulose solubilization and confirmed by post-hydrolysis with dilute acid (Sluiter et al., 2010). First hour (initial hydrolysis rate) and 24 h glucose and cellulose oligomer release patterns of partially hydrolyzed cellulose were monitored for various loadings of single enzyme components (CBH1 and EG2) and their combinations. Sugar release during cellulose hydrolysis by single or mixed CBH1 and EG2 were calculated as a percentage of total loaded cellulose. The degree of synergism (DOS) is defined by Equation (2).

$$\text{DOS} = \frac{Y_{\text{CBH1+EG2}}}{Y_{\text{CBH1}} + Y_{\text{EG2}}} \quad (2)$$

in which, $Y_{\text{CBH1+EG2}}$ is the sugar released by CBH1 and EG2 mixtures and Y_{CBH1} and Y_{EG2} are the sugar released by individual CBH1 and EG2, respectively.

Results

Generation of Partially Hydrolyzed Cellulose

Enzymatic hydrolysis of micro-crystalline cellulose (MCC, trademark name: Avicel) was interrupted at 1, 2, 4, 5, and 15 h to result in 28%, 41%, 68%, 74%, and 81% cellulose conversion, as shown in Table I. Table I also shows that the incremental hydrolysis rate was virtually constant when hydrolysis was "restarted" with solids from each stage of partial hydrolysis. This is in general agreement with previous studies by Yang et al. (2006). In addition, the reducing end content of untreated and partially hydrolyzed cellulose reported in Table I showed no statistical differences over 0–15 h.

The data in Table I also show that small changes were measured in the CrI of partially hydrolyzed cellulose over the entire 15 h hydrolysis period compared with untreated Avicel. For instance, 1 h of partial cellulose hydrolysis (28% conversion) increased the CrI slightly from 65.1% for untreated Avicel (0% conversion) to about 70%, suggesting amorphous cellulose removal. However, the CrI of cellulose interrupted at 2–5 h (41–74% conversion) stayed about the same, while the CrI of cellulose interrupted after 15 h (81% conversion) dropped slightly, likely due to significant crystalline cellulose deconstruction during digestion.

Characterization of Partially Hydrolyzed Cellulose

Spectrometric and microscopic techniques were used to investigate the compositional and surface morphological characteristics of untreated and partially converted cellulose samples. Figure S1 summarizes ATR-FTIR spectra, while Figure S2 shows the FT-Raman spectra of untreated and partially converted cellulose. FTIR and FT-Raman spectra confirmed a slight crystallinity increase as enzymatic hydrolysis proceeds, but no significant changes in band intensities were observed at 1056 cm^{-1} (C–O stretch in cellulose). However, the peak intensity of the C–O vibration of the crystalline cellulose (around 1098 cm^{-1} in FTIR spectra) in partially hydrolyzed cellulose samples (28–81% conversion) increased from that for untreated cellulose. The spectra obtained from partially hydrolyzed cellulose clearly show an increase of the crystalline cellulose band at 1098 cm^{-1}, while the amorphous band at 900 cm^{-1} remained nearly unchanged, confirming a slight increase in crystallinity compared with untreated cellulose as measured by XRD.

Differences in FT-Raman spectra between untreated and partially hydrolyzed cellulose suggest that the hydrogen bonding patterns differed in each of these cellulose samples. In the low frequency region (600–250 cm^{-1}), there were only minor differences between the spectra of 28%, 41%, 68%, 74%, and 81% converted cellulose, but the peaks in the untreated cellulose spectrum were narrower and better resolved, probably due to the uniform vibration energy associated with the larger crystallites size of the untreated cellulose. The most notable difference between the untreated and partially hydrolyzed cellulose spectra in the low frequency region was the ratio of peak intensities at 913 and 1056 cm^{-1} ($I_{913/1056}$). These ratios were higher for the spectrum of untreated cellulose than for partially hydrolyzed cellulose and appear to be inversely correlated with crystallinity and cellulose DP (Wiley and Atalla, 1987). The ratio of peak intensity of 381–1091 cm^{-1} has been previously used to determine crystallinity (Agarwal et al., 2013), and disappearance of the 381 cm^{-1} peak indicates a reduction in amorphous cellulose and increase in crystallinity in partially hydrolyzed cellulose samples. In the O–H stretching region (3200–3600 cm^{-1}), the notable differences between untreated and partially hydrolyzed cellulose reflect plausibly different hydrogen bonding patterns among these samples (Agarwal et al., 2013).

Figure 1 reveals the surface morphology and ultra-structure of partially hydrolyzed cellulose imaged by atomic force microscopy

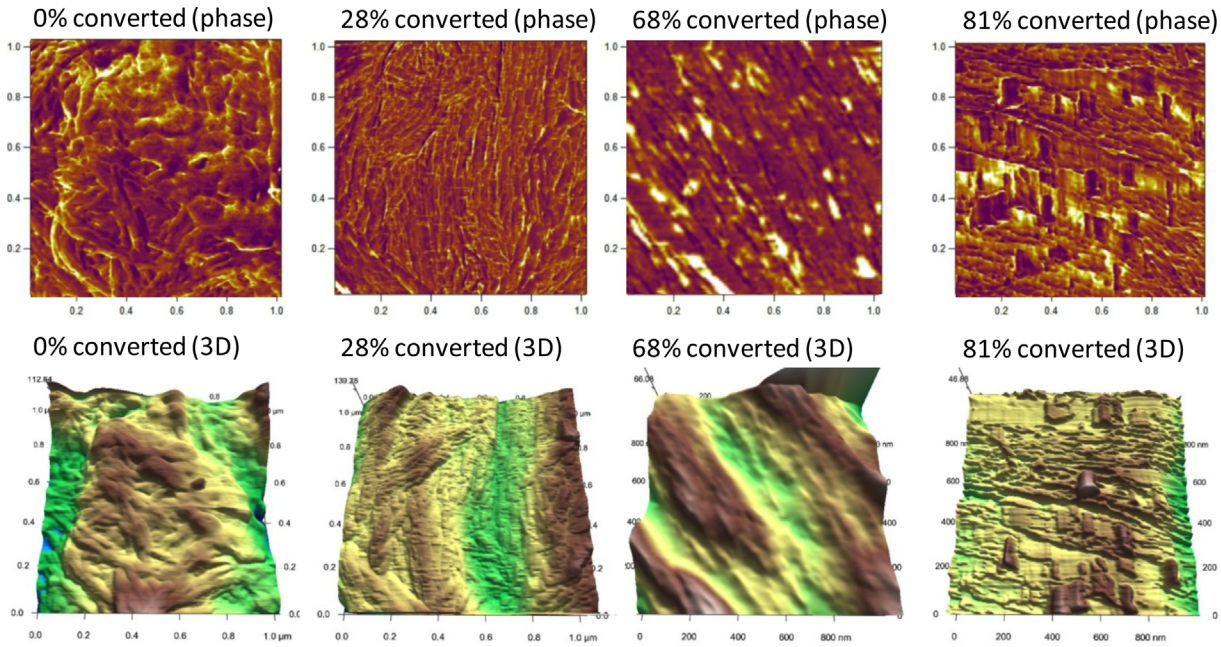

Figure 1. Surface morphology and ultra-structure of partially converted cellulose imaged by atomic force microscopy (AFM) with a representative image field of $1.0 \times 1.0\ \mu m^2$ to show both phase and 3D topography images.

(AFM) with a representative image field of $1.0 \times 1.0\ \mu m^2$. The phase images provide better contrast in surface morphology, while the 3D topography images reveal the relative roughness of the scanned surface. The AFM scan of untreated cellulose (0% converted) revealed both highly ordered fiber bundles and an amorphous structure. However, AFM scans of the partially hydrolyzed cellulose (28% converted) revealed slightly etched surfaces and edges and highly etched surface and edges (68% converted). The AFM scan of the near-completely converted (81%) cellulose showed deeply etched surfaces and edges and some isolated fractions of cellulose hydrolysis residuals. The root mean square (RMS) surface roughness was also calculated from the 3D topography images. For untreated cellulose, the RMS roughness was approximately 29.9 ± 5.4 nm, while for 28% converted cellulose, the RMS roughness stayed approximately the same at about 30.3 ± 6.1 nm. However, RMS roughness of the cellulose surface dropped to 19.3 ± 3.3 nm and 8.1 ± 1.1 nm with 68% and 81% conversion, respectively. The reduced surface roughness could be due to hydrolysis removing top layers that include randomly distributed cellulose microfibers and the amorphous region to expose more ordered and packed crystalline cellulose.

CBH1 and EG2 Adsorption on Partially Hydrolyzed Cellulose

Enzyme adsorption is plotted against CBH1 and EG2 loadings of 0–2.5 μmol/g cellulose for loading of CBH1 and EG2 alone in Figure 2 or together in equal molar amounts in Figure 3 to partially hydrolyzed cellulose. The results in Table I show that the cellulose adsorption capacity of CBH1 and EG2 rapidly dropped as cellulose hydrolysis progressed, while the hydrolysis rate remained fairly constant. The enzyme adsorption capacity also dropped as enzymatic hydrolysis proceeded when CBH1 and EG2 were loaded together at equal molar concentrations. Interestingly, the sums of enzyme capacities of CBH1 and EG2 when loaded together were similar to the adsorption capacity of individual enzymes when loaded separately. In addition, results showed that EG2 occupied more adsorption sites than CBH1 when loaded at similar molar concentrations, although CBH1 is dominant in natural cellulases systems, such as from *T. reesei*. The adsorption parameters calculated based on the Langmuir model, that is, the maximum cellulase adsorption capacity, σ, and equilibrium constant, k_d, are listed in Table II. These results show that the CBH1 adsorption capacity dropped dramatically from 1.02 μmol/g cellulose for untreated Avicel to 0.59 μmol/g cellulose for 28% converted cellulose and then dropped gradually from 0.52 to 0.37 μmol/g as hydrolysis continued to 41–81% cellulose conversion. Similar trends can be seen for EG2 adsorption on partially hydrolyzed cellulose. However, in general agreement with many previous reports, the EG2 adsorption capacity was higher than for CBH1 (Medve et al., 1994). For instance, the EG2 adsorption capacity for unconverted cellulose of 1.63 μmol/g cellulose was much higher than the value of 1.02 μmol/g cellulose measured for CBH1.

When CBH1 and EG2 were added at the same time, adsorption capacities of both enzymes were much lower than when they were applied alone. As shown in Table II, CBH1 and EG2 adsorption capacities to unconverted cellulose were 0.40 and 0.71 μmol/g cellulose, respectively, which are only about 50% of their adsorption

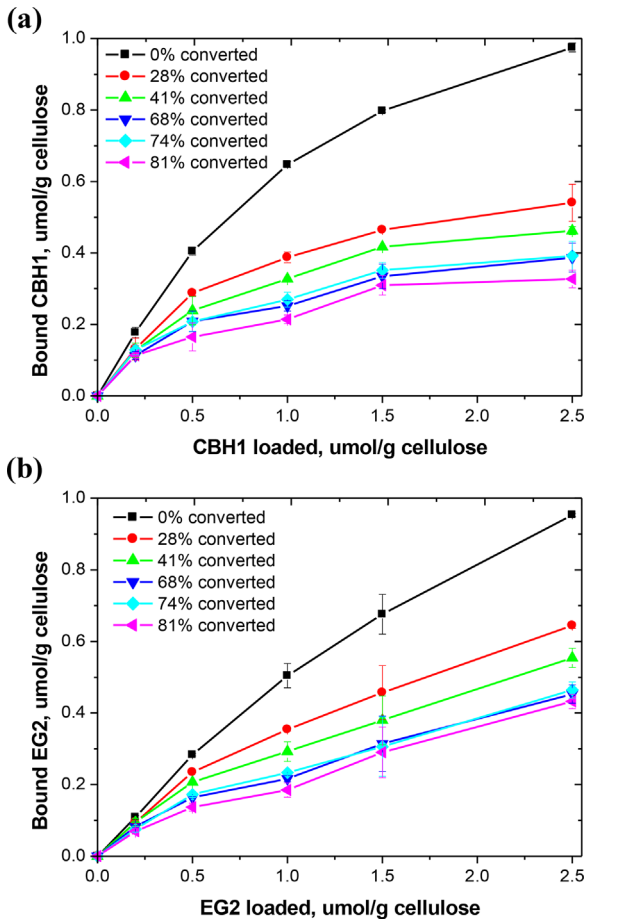

Figure 2. Isothermal binding of individual CBH1 and EG2 enzymes on partially hydrolyzed micro-crystalline cellulose (MCC, Avicel)

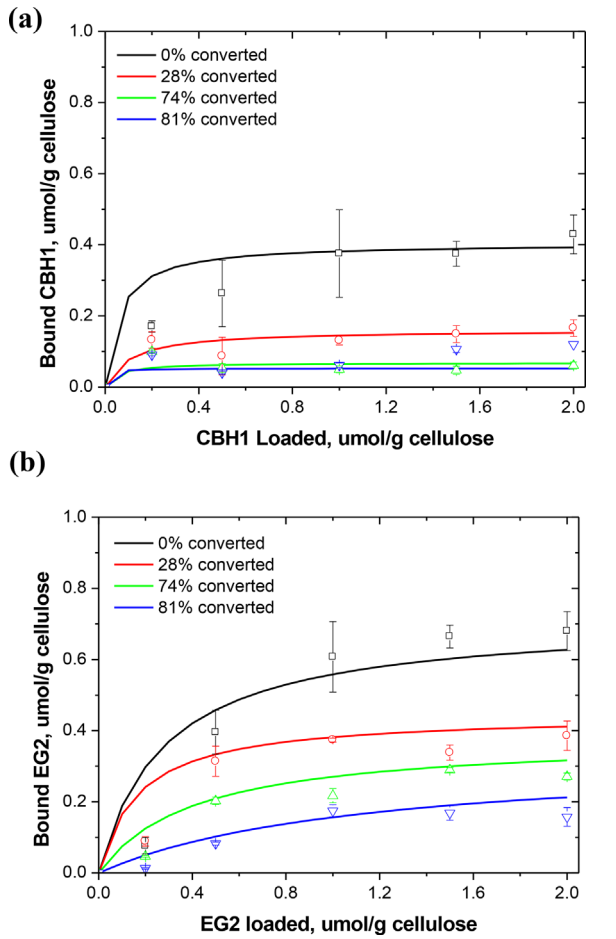

Figure 3. Synergistic isothermal binding of (**a**) CBH1 and (**b**) EG2 on partially hydrolyzed micro-crystalline cellulose (MCC, Avicel) when equal molar amounts of the two enzymes were loaded together.

capacities when they were loaded alone. As hydrolysis proceeded, both CBH1 and EG2 adsorption capacities dropped. For example, CBH1 adsorption capacity dropped from 0.40 μmol/g on unconverted cellulose to 0.16 μmol/g on 28% converted cellulose and further to 0.05 μmol/g on the 81% converted cellulose produced after 15 h of hydrolysis. The drop in adsorption capacity provided evidence for depletion of binding sites for both CBH1 and EG on cellulose surfaces as hydrolysis proceeded. In addition, competition for binding sites or enzyme crowding could also lead to the reduction in adsorption capacity (Levine et al., 2010). Moreover, the CBH1 adsorption capacity was much lower than that of EG2, and the difference grew as hydrolysis proceeded, irrespective of whether these enzymes were added alone or together. As shown in Table I, the ratio of the maximum cellulase adsorption capacity σ of EG2 to that of CBH1 increased from 1.60 for unconverted cellulose to 3.13 for 81% converted cellulose. Similarly, when CBH1 and EG2 were loaded together in equal molar amounts, the σ ratio of EG2:CBH1 increased from 1.77 with unconverted cellulose to 6.33 with 81% converted cellulose, probably because more binding sites for EG2 became available as hydrolysis proceeded (Medve et al., 1998).

Substrate Reactivity as Revealed by 1st Hour Hydrolysis Rate

Figure 4 reports sugar yields produced during the 1st hour of hydrolysis of partially hydrolyzed cellulose to measure how the hydrolysis rate changes for CBH1 and EG2 alone at low (0.1 μmol/g cellulose), high (1.0 μmol/g cellulose), and together in equal molar enzyme loadings, respectively. In general, larger amounts of glucose and cellulose oligomers were released when cellulose was hydrolyzed by CBH1 alone than by EG2 alone. For example, at enzyme loading of 0.1 μmol/g cellulose, CBH1 hydrolyzed about 1.5–2.3% of the initial cellulose to glucose while EG2 liberated only 0.4–1.1% in the same 1 h period. Similarly, at an enzyme loading of 1.0 μmol/g cellulose, CBH1 solubilized about 3.2–5.7% of the initial cellulose while EG2 only released 1.0–1.2%. When the two enzymes were loaded together, sugar yields increased from that measured for the individual enzyme due to the synergy between exo- and endo-glucanases.

Further examination of the sugar profiles in Figure 4 shows that adding CBH1 alone primarily released glucose, cellobiose,

Table II. Adsorption capacities of CBH1 and EG2 on interrupted Avicel when loaded individually or together in equal molar amounts.

	CBH1 alone		EG2 alone		EG2/CBH1	CBH1 synergistic		EG2 synergistic		EG2/CBH1
	σ	R^2	σ	R^2	σ Ratio	σ	R^2	σ	R^2	σ Ratio
0 h	1.02	0.99	1.63	0.99	1.60	0.40	0.92	0.71	0.85	1.77
1 h	0.59	0.98	0.98	0.99	1.68	0.16	0.91	0.45	0.94	2.78
2 h	0.52	0.98	0.86	0.97	1.65	ND	ND	ND	ND	ND
4 h	0.42	0.97	0.83	0.99	1.96	ND	ND	ND	ND	ND
5 h	0.42	0.96	0.81	0.96	1.93	0.07	0.89	0.38	0.90	5.58
15 h	0.37	0.95	1.17	0.96	3.13	0.05	0.76	0.33	0.89	6.33

σ, maximum adsorption capacities, μmol/g cellulose; R^2, coefficient of determination; ND, not determined.

and DP>3 cellodextrins. For example, at a CBH1 loading of 1.0 μmol/g cellulose, about equal amounts of glucose and cellobiose (1% each) were released, while DP>3 cellodextrins accounted for 2–3% of the iniital cellulose. However, adding EG2 alone mostly released DP>3 cellodextrins and very low levels of glucose and cellobiose. These observations are in line with CBH1 mainly attacking reducing ends of cellulose to release cellobiose and glucose and EG2 randomly attacking the middle of cellulose chains to release higher DP cellodextrins (Medve et al., 1994). Adding the two enzymes at the same time released mostly glucose, a smaller portion of DP>3 cellodextrins, and little cellobiose due to exo–endo synergism. Ratios of cellobiose/(glulose + cellotriose) in the sugar products during 1st hour of hydrolysis were calculated (Table SII) as an indicator of processivity (Nakamura et al., 2014). It is shown that the ratios of cellobiose/(glucose + cellotriose) were affected by both the CBH1 and EG2 loading/combination and the substrate, suggesting that the processivity correlates to both factors.

Equilibrium Sugar Release as Revealed by 24 h Hydrolysis

The 24 h sugar yields in Figure 5 provide another measure of the effectiveness of CBH1 and EG2 and their combinations. First, we can see that substantial sugar release occurred between 1 and 24 h of hydrolysis of partially hydrolyzed cellulose samples, especially when CBH1 and EG2 were loaded together. For instance, a CBH1 loading of 0.1 μmol/g cellulose hydrolyzed approximately 3–5% of the cellulose to sugars, primarily in the forms of cellobiose and DP>3 cellodextrins. The primary sugars released by EG2 were DP>3 cellodextrins with small portion of glucose and cellobiose at an EG2 loading of 0.1 or 1.0 μmol/g cellulose; however, the approximately 1–3% of cellulose hydrolyzed to sugars by EG2 was lower than that by CBH1. Adding CBH1 and EG2 together converted as much as 15% and 27% of the cellulose into sugars (with over 50% of DP>3 cellodextrins) at enzyme loadings of 0.1 and 1.0 μmol/g cellulose of each enzyme, respectively. Furthermore, as a general trend, less sugar was released from hydrolysis of 28–81% converted cellulose than that from unconverted cellulose, consistent with their reduced absorption capacities (Table II). Low absorption capacities resulting from "depletion" of binding sites along with accumulation of DP>3 oligosaccharides may contribute to the drop in sugar release, especially at lower enzyme loadings or with unbalanced enzyme mixtures.

DOS

Figure 6 shows how the DOS between CBH1 and EG2 changes with cellulose conversion at enzyme loadings of 0.1 and 1.0 μmol/g cellulose, respectively. In general, a DOS greater than 1.0 indicates synergy between CBH1 and EG2, while a DOS less than 1.0 results from competition between CBH1 and EG2 when loaded together. An enzyme loading of 0.1 μmol/g cellulose resulted in a DOS of 1.4 for hydrolysis of untreated Avicel (0% conversion) during the 1st hour (Fig. 6a), but the synergism dropped to approximately one for the 1st hour of hydrolysis of partially converted cellulose (28–81% conversion), indicating reduced synergy between CBH1 and EG2. However, DOS increased substantially to 1.9 for 24-h hydrolysis of untreated Avicel (0% converted) and leveled off to ∼1.5–1.7 for 28–81% converted cellulose samples, demonstrating strong synergistic effects between CBH1 and EG2 (Fig. 6b). Interestingly, for all but untreated Avicel (0% converted), the DOS for partially hydrolyzed cellulose dropped to about 0.75 at a CBH1 and EG2 loading of 1.0 μmol/g cellulose, indicating competition of CBH1 and EG2 (Fig. 6c). Furthermore, at the 24-h hydrolysis time, the DOS for the CBH1 and EG2 loading of 1.0 μmol/g cellulose leveled off at ∼1.0, a much lower value than for CBH1 and EG2 loadings at 0.1 μmol/g cellulose (Fig. 6d). These results indicate that high CBH1 and EG2 loadings may result in enzyme crowding or competition that limits both enzyme adsorption to cellulose and the sugar release.

Discussion

Many kinetic studies report that the cellulose hydrolysis rate by cellulases drops during cellulose hydrolysis, due to an array of factors (Mansfield et al., 1999; Yang et al., 2011), and "Interrupt" and "restart" experiments have been employed to identify factors that affect cellulose hydrolysis (Desai and Converse, 1997; Zhang et al., 1999). A "restart" experiment washes away sugars and intermediate hydrolysis products and the attached cellulases from partially hydrolyzed cellulose surface and introduces fresh enzymes to the washed substrates. The washing procedure usually applies harsh chemicals or solvents that may also cause irreversible alteration of the substrates (Hong et al., 2007; Zhu et al., 2009). To minimize such possibilities, this study applied proteinase treatment to remove cellulases followed by proteinase inhibitors to deactivate the proteinase before restarting cellulose hydrolysis at original conditions (Yang et al., 2006). Thus, adding enzymes to these "restarted" samples gives a picture of how reactivity of the cellulose shifts with

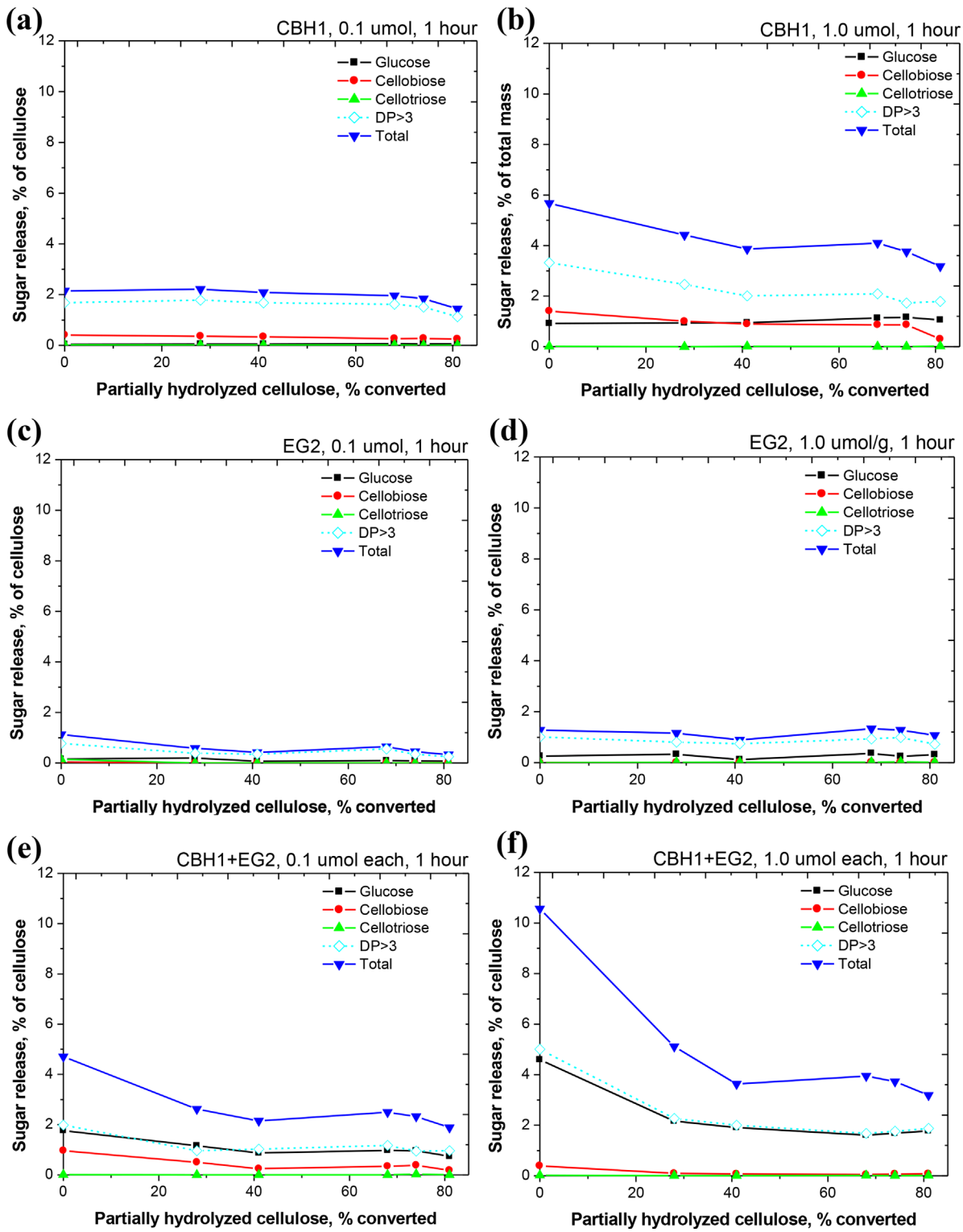

Figure 4. Sugar release after 1 h of hydrolysis of partially hydrolyzed/converted cellulose at 0.1 and 1.0 μmol/g of CBH1 and EG2 loaded alone or together: (**a**) CBH1 alone at 0.1 μmol/g cellulose, (**b**) CBH1 alone at 1.0 μmol/g cellulose, (**c**) EG2 alone at 0.1 μmol/g cellulose, (**d**) EG2 alone at 1.0 μmol/g cellulose, (**e**) CBH1 + EG2 together at 0.1 μmol/g cellulose each, and (**f**) CBH1 + EG2 together at 1.0 μmol/g cellulose each.

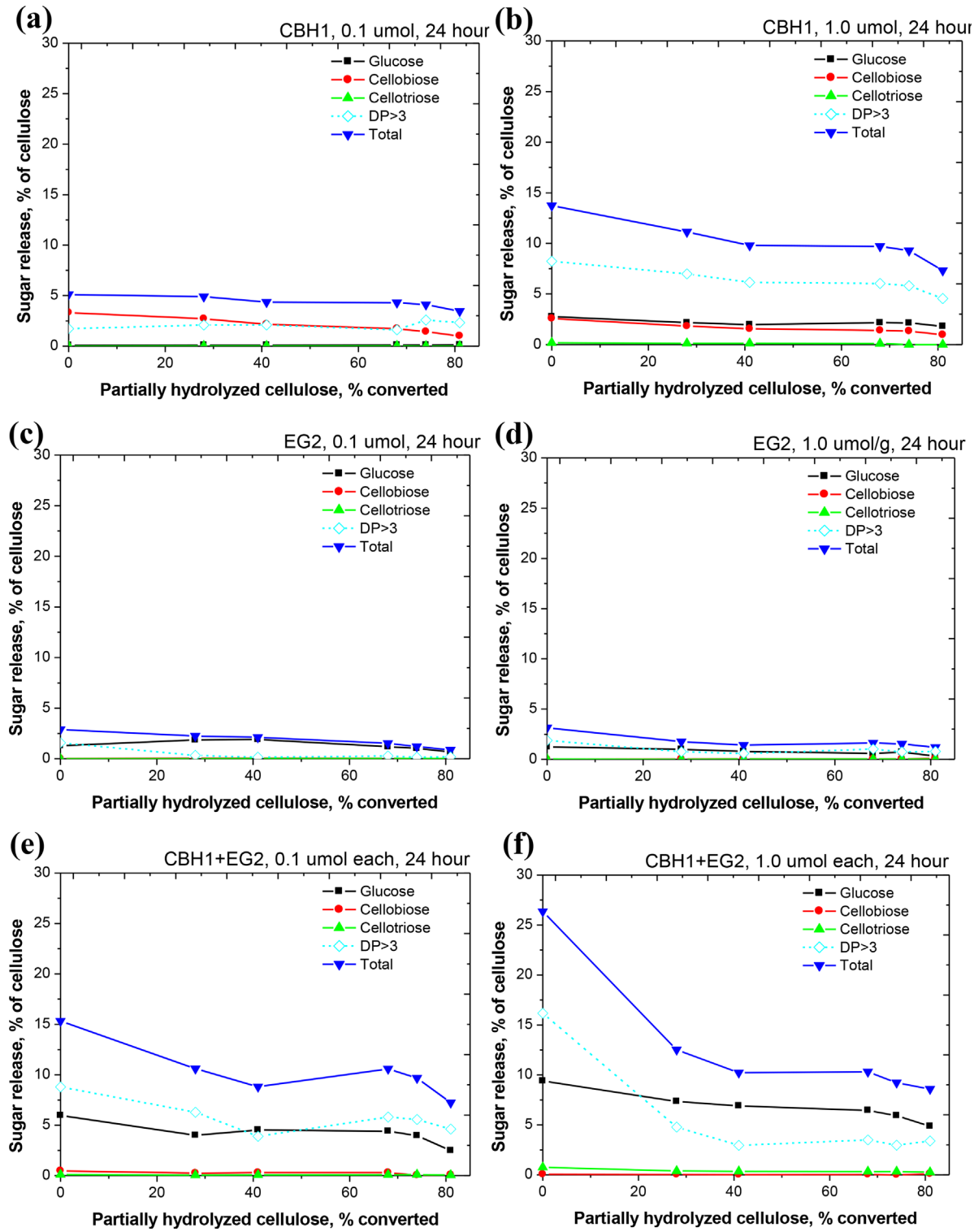

Figure 5. Sugar release after 24 h of hydrolysis of partially hydrolyzed/converted cellulose at 0.1 and 1.0 μmol/g of CBH1 and EG2 loaded alone or together: (**a**) CBH1 alone at 0.1 μmol/g cellulose, (**b**) CBH1 alone at 1.0 μmol/g cellulose, (**c**) EG2 alone at 0.1 μmol/g cellulose, (**d**) EG2 alone at 1.0 μmol/g cellulose, (**e**) CBH1 + EG2 together at 0.1 μmol/g cellulose each, and (**f**) CBH1 + EG2 together at 1.0 μmol/g cellulose each.

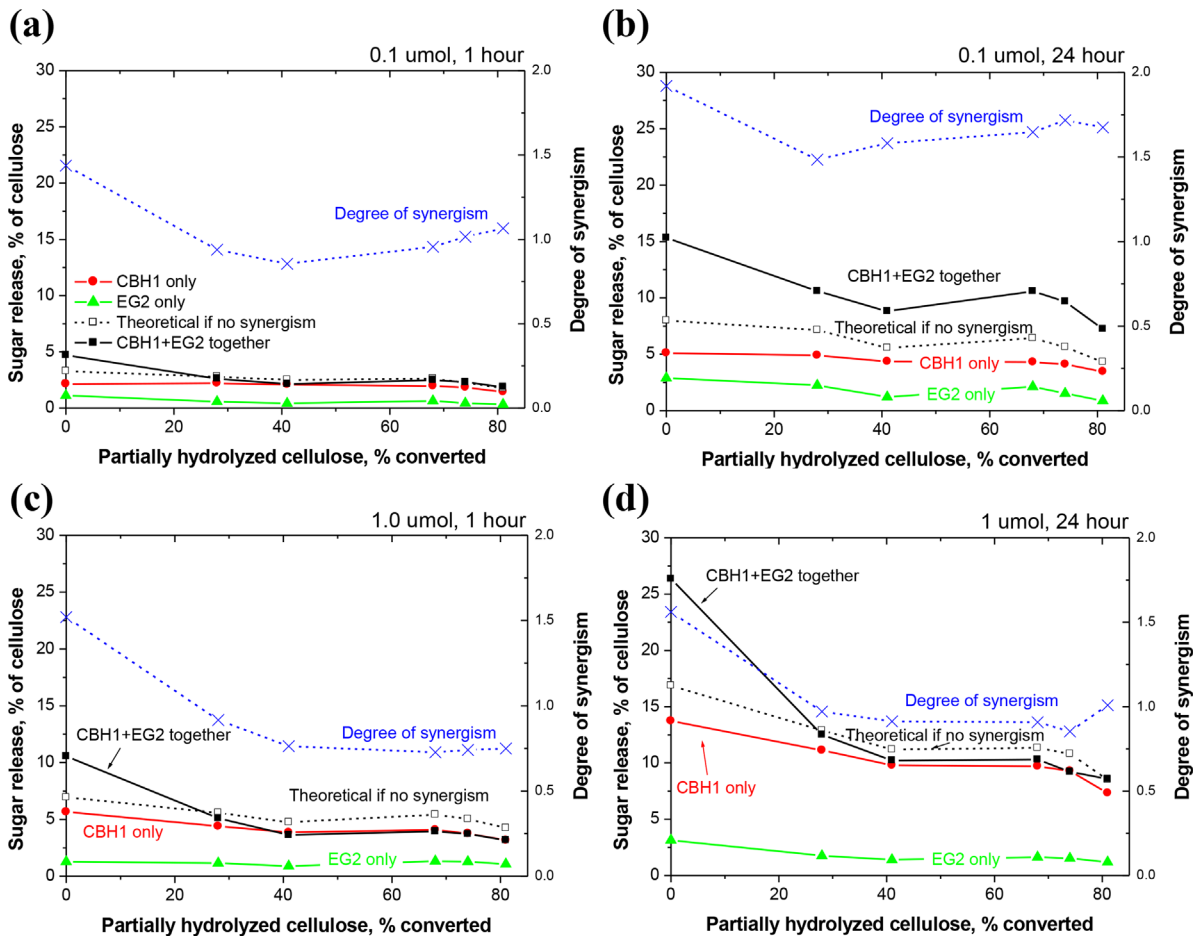

Figure 6. Degree of synergy changes with cellulose conversion: (**a**) CBH1 + EG2 each at 0.1 μmol/g for 1 h, (**b**) CBH1 + EG2 each at 0.1 μmol/g for 24 h, (**c**) CBH1 + EG2 each at 1.0 μmol/g for 1 h, and (**d**) CBH1 + EG2 each at 1.0 μmol/g for 24 h.

conversion due to changes in the substrate that is independent of loss of enzyme activity or mobility and facilitates understanding dynamic interactions between enzyme and cellulose.

Cellulose substrates (e.g., Avicel) are usually not structurally uniform, and cellulases have different affinities and reactivities with crystalline and amorphous portions. The resulting solid substrates interrupted during cellulose hydrolysis have different characteristics due to creation of new cellulose chain ends by endoglucanases and cleavage of cellulose chains by exoglucanases (Kostylev et al., 2012). Cellulose crystallinity has long been thought to play an important role in enzymatic hydrolysis. However, the reported changes in CrI after enzymatic hydrolysis have not shown a clear correlation to sugar yields (Park et al., 2010). Even though studies have produced evidence to support CrI increases during enzymatic hydrolysis (Wang et al., 2006), the increases reported have often been small, in line with the observation in this study. For instance, Chen et al. (2007) measured only a 2.6% increase in CI after 18% conversion of bacterial cellulose, while Wang et al. (2006) reported only a 2.0% increase in CrI after 6 days of hydrolysis of cotton fibers by crude cellulases. Nevertheless, other studies suggested that the CrI of partially hydrolyzed cellulose could drop due to breakdown of cellulose chains into more random arrangements (Park et al., 2010). However, the initial increase and subsequent drop in CrI reported in our paper indicates a dynamic hydrolysis process that favors digestion of the amorphous cellulose component at the start of conversion followed by shifting to breakdown of crystalline cellulose structures. However, no direct evidence can be gathered as to whether there is a preferential digestion of amorphous or crystalline cellulose regions.

Recent developments in high-resolution/high-speed atomic force microscopy (AFM) offer potential tools to reveal the surface morphology and physical proximity of substrate-enzyme reactions (Igarashi et al., 2009, 2011). AFM imaging of both highly ordered fiber bundles and amorphous structures in this study provided direct evidence of cellulose surface morphology becoming flatter at the1 μm scale as enzymatic hydrolysis of Avicel proceeded (Fig. 1). Interestingly, AFM scans of partially converted cellulose (28% conversion) also revealed slightly etched surfaces and edges and increased roughness of surface. AFM scans of the near-completely converted cellulose revealed much greater etching of surfaces and edges and less surface roughness. The AFM observations in combination with FTIR and FT-Raman

provide evidence of the dynamic enzyme action changing the surface morphology and structure. These altered surface features may greatly impact enzyme adsorption on cellulose and enzyme processability for sugar release.

Enzymatic hydrolysis of cellulose is a multiphase reaction in which cellulases attack solid substrate surfaces to release soluble sugars monomers and oligomers with subsequent hydrolysis to sugar monomers taking place in the liquid phase. The necessary adsorption of cellulase on the solid substrate prior to hydrolysis beginning requires recognition of a binding site by cellulases followed by physical absorption to cellulose (Beldman et al., 1987; Ståhlberg et al., 1991, 1993). Therefore, substrate features greatly affect cellulase adsorption (Beguin and Aubert, 1994). Results from this study showing a clear trend of reduced adsorption of both CBH1 and EG2 when they were loaded alone on partially hydrolyzed cellulose compared to that of untreated Avicel cellulose indicates that the overall number of available binding sites drops as hydrolysis progresses or the substrate becomes less accessible to enzymes. Moreover, the adsorption capacity declined even further when CBH1 and EG2 were loaded together, possibly because of competition for binding sites on the cellulose substrate. Similar phenomenon has been reported previously for CBH1/CBH2 or CBH1/EG2 combinations (Medve et al., 1994, 1998). It is also noticed that the coefficient of determination (R^2) is low for the synergistic adsorption of CBH1 and EG2 when adsorption data were fit into Langmuir equation. A recent study suggested that the Hill's model was superior to Langmuir model for synergy experiments probably due to changes of cooperativity (the steric exclusion effect) when both CBH1 and EG2 were loaded (Sugimoto et al., 2012). This observation may also tie to the enzyme "crowding" as supported experimentally from this study and a recent modeling work (Levine et al., 2010).

Interestingly, in addition to the adsorption capacities of CBH1 and EG2 dropping with conversion, the ratio of bound EG2 and CBH1 also changed. High concentrations of EG2 alone bound to untreated Avicel cellulose to a considerably higher extent than CBH 1, consistent with a previous finding (Medve et al., 1998). Furthermore, the two enzymes competed for binding sites when loaded together at a high loading, that is, binding of EG2 was significantly affected by CBH 1, and vice versa. For the first time, results from this study revealed that the adsorption capacity ratio of EG2 to CBH1 increased as cellulose hydrolysis progressed even though the overall binding capacity dropped. Two mechanisms could, in principle, explain the lower adsorption of EG2 or CBH1: (i) CBH 1 hydrolyzes EG2's binding sites ("depletion") or (ii) CBH 1 occupies EG2's binding sites ("competition"). Enzyme "crowding" or "jamming" could also be responsible for a drop in cellulase adsorption and hydrolysis rates (Bansal et al., 2009; Bonsal et al., 2012). Results from this study experimentally support results of recent modeling work that predict enzyme crowding is more apparent for low surface areas (Levine et al., 2010). Additional analysis indicates that both the CBH1 and EG2 loading/combination and the substrate affect the ratios of cellobiose/(glucose + cellotriose) in the hydrolysis products, suggesting that the processivity correlates to both factors, in agreement of a recent study correlating the ratio with the actual processivity measured by HS-AFM (Nakamura et al., 2014).

Although synergism among *Trichoderma* cellulase components has been greatly studied (Beldman et al., 1988; Jeoh et al., 2006; KlemanLeyer et al., 1996), the results are often contradictory. A primary reason for such inconsistencies probably results from differences in substrates and experimental conditions and variations in enzyme purity (Reinikainen et al., 1995). Nonetheless, it is apparent that synergism depends on the ratio of the individual enzymes, substrate saturation, and physicochemical and surface properties of the substrate (Henrissat et al., 1985; Nidetzky et al., 1993). The results reported here reveal some interesting insights into the synergistic action of CBH1 and EG2 on partially hydrolyzed cellulose. During the first hydrolysis hour, the DOS of CBH1 and EG2 was greater than one only for untreated Avicel (0% converted) regardless of enzyme loading. However, the DOS dropped significantly for partially hydrolyzed cellulose, especially at a high enzyme loading (1.0 μmol/g cellulose). These results are supported by previous findings that the degree of synergistic effects between binary exo/endo *Thermobifida fusca* cellulases mixtures was sensitive to enzyme loadings (Jeoh et al., 2006). Furthermore, EG2-CBH1 synergies have been proposed to be most evident at sufficiently high cellulose surface areas (Levine et al., 2010), and synergism drops as the available substrate surface area becomes low (Igarashi et al., 2009, 2011).

Conclusions

A "restart" protocol was applied to identify factors that control the rate of cellulose hydrolysis by enzymes. For the first time, our results revealed dynamic profiles for enzyme adsorption, sugar release, and oligosaccharide yields over time for interrupted enzymatic hydrolysis of Avicel by purified CBH1 and EG2 enzyme components and their combinations. When the enzymes were applied individually, CBH1 and EG2 adsorption capacities dropped rapidly with conversion and then leveled off likely due to the "depletion" of binding sites as cellulose was progressively hydrolyzed. Sugar release patterns generally correlated well with enzyme adsorption on untreated and partially hydrolyzed cellulose. Moreover, these results suggest that more oligosaccharides (DP>3 cellodextrins) than soluble sugars could be produced during cellulose hydrolysis and that both cellulose substrate and enzyme loadings and combinations influenced sugar time release profiles. Further investigation of such aspects as oligomer distributions, effective enzyme binding capacities, and depolymerization equilibration will help aid in understanding cellulase–cellulose interactions and factors governing cellulose reactivity. This study also suggests that kinetic models of cellulose hydrolysis should include correlating cellulose reactivity, oligosaccharide distribution, the effective enzyme binding capacity, and equilibration of depolymerization in order to fully understand enzymatic hydrolysis of cellulose.

Research conducted by the BioEnergy Science Center (BESC) and Joint BioEnergy Institute (JBEI) was supported by Office of Biological and Environmental in the Office of Science of the U.S. Department of Energy under Contract Numbers DE-PS02-06ER64304 and DE-AC02-05CH11231, respectively. We also acknowledge the Center for Environmental Research and Technology (CE-CERT) of the Bourns College of Engineering for

providing the facilities and the Ford Motor Company for funding the Chair in Environmental Engineering that facilitates projects such as this one. Work at WSU was partially funded by DARPA Young Faculty Award contract # N66001-11-1-414, and the authors acknowledge the Bioproducts, Sciences and Engineering Laboratory and Department of Biosystems Engineering at Washington State University for providing facilities and equipment to perform our research. We acknowledge the National Science Foundation under Cooperative Agreement No. 1355438 for partial support of the effort at University of Kentucky. We acknowledge Xiaodi Gao for assisting enzyme adsorption experiments. We thank Drs. Edmund Larenas and Colin Mitchinson from Genencor, a Danisco Division (now DuPont Industrial Biosciences) for generously providing purified CBH1 and EG2 enzymes and offering valuable suggestions to this research.

References

Agarwal UP, Zhu JY, Ralph SA. 2013. Enzymatic hydrolysis of loblolly pine: Effects of cellulose crystallinity and delignification. Holzforschung 67(4):371–377.

Bansal P, Hall M, Realff MJ, Lee JH, Bommarius AS. 2009. Modeling cellulase kinetics on lignocellulosic substrates. Biotechnol Adv 27(6):833–848.

Beguin P, Aubert JP. 1994. The biological degradation of cellulose. FEMS Microbiol Rev 13(1):25–58.

Beldman G, Voragen AGJ, Rombouts FM, Pilnik W. 1988. Synergism in cellulose hydrolysis by endoglucanases and exoglucanases purified from trichoderma-Viride. Biotechnol Bioeng 31(2):173–178.

Beldman G, Voragen AGJ, Rombouts FM, Searlevanleeuwen MF, Pilnik W. 1987. Adsorption and kinetic-behavior of purified endoglucanases and exoglucanases from Trichoderma-viride. Biotechnol Bioeng 30(2):251–257.

Bonsal P, Vowell BJ, Hall M, Realff MJ, Lee JH, Bommarius AS. 2012. Elucidation of cellulose accessibility, hydrolysability and reactivity as the major limitations in the enzymatic hydrolysis of cellulose. Bioresour Technol 107:243–250.

Chen Y, Stipanovic AJ, Winter WT, Wilson DB, Kim YJ. 2007. Effect of digestion by pure cellulases on crystallinity and average chain length for bacterial and microcrystalline celluloses. Cellulose 14(4):283–293.

Desai SG, Converse AO. 1997. Substrate reactivity as a function of the extent of reaction in the enzymatic hydrolysis of lignocellulose. Biotechnol Bioeng 56(6):650–655.

Eriksson T, Karlsson J, Tjerneld F. 2002. A model explaining declining rate in hydrolysis of lignocellulose substrates with cellobiohydrolase I (Cel7A) and endoglucanase I (Cel7B) of Trichoderma reesei. Appl Biochem Biotechnol 101:41–60.

Henrissat B, Driguez H, Viet C, Schulein M. 1985. Synergism of cellulases from trichoderma-Reesei in the degradation of cellulose. Bio-Technology 3(8):722–726.

Himmel ME, Ding S-Y, Johnson DK, Adney WS, Nimlos MR, Brady JW, Foust TD. 2007. Biomass recalcitrance: Engineering plants and enzymes for biofuels production. Science 315(5813):804–807.

Himmel ME, Ruth MF, Wyman CE. 1999. Cellulase for commodity products from cellulosic biomass. Curr Opin Biotechnol 10(4):358–364.

Hong J, Ye X, Zhang YHP. 2007. Quantitative determination of cellulose accessibility to cellulase based on adsorption of a nonhydrolytic fusion protein containing CBM and GFP with its applications. Langmuir 23(25):12535–12540.

Igarashi K, Koivula A, Wada M, Kimura S, Penttila M, Samejima M. 2009. High speed atomic force microscopy visualizes processive movement of trichoderma reesei cellobiohydrolase I on crystalline cellulose. J Biol Chem 284(52):36186–36190.

Igarashi K, Uchihashi T, Koivula A, Wada M, Kimura S, Okamoto T, Penttila M, Ando T, Samejima M. 2011. Traffic jams reduce hydrolytic efficiency of cellulase on cellulose surface. Science 333(6047):1279–1282.

Jeoh T, Wilson DB, Walker LP. 2002. Cooperative and competitive binding in synergistic mixtures of Thermobifida fusca cellulases Ce15A, Ce16B, and Ce19A. Biotechnol Prog 18(4):760–769.

Jeoh T, Wilson DB, Walker LP. 2006. Effect of cellulase mole fraction and cellulose recalcitrance on synergism in cellulose hydrolysis and binding. Biotechnol Prog 22(1):270–277.

KlemanLeyer KM, SiikaAho M, Teeri TT, Kirk TK. 1996. The cellulases endoglucanase I and cellobiohydrolase II of Trichoderma reesei act synergistically to solubilize native cotton cellulose but not to decrease its molecular size. Appl Environ Microbiol 62(8):2883–2887.

Kostylev M, Moran-Mirabal JM, Walker LP, Wilson DB. 2012. Determination of the molecular states of the processive endocellulase Thermobifida fusca Cel9A during crystalline cellulose depolymerization. Biotechnol Bioeng 109(1):295–299.

Larsen KL, Barsberg S. 2010. Theoretical and raman spectroscopic studies of phenolic lignin model monomers. J Phys Chem B 114(23):8009–8021.

Levine SE, Fox JM, Blanch HW, Clark DS. 2010. A mechanistic model of the enzymatic hydrolysis of cellulose. Biotechnol Bioeng 107(1):37–51.

Mansfield SD, Mooney C, Saddler JN. 1999. Substrate and enzyme characteristics that limit cellulose hydrolysis. Biotechnol Prog 15(5):804–816.

Medve J, Karlsson J, Lee D, Tjerneld F. 1998. Hydrolysis of microcrystalline cellulose by cellobiohydrolase I and endoglucanase II from Trichoderma reesei: Adsorption, sugar production pattern, and synergism of the enzymes. Biotechnol Bioeng 59(5):621–634.

Medve J, Stahlberg J, Tierneld F. 1994. Adsorption and synergism of cellobiohydrolase-I and cellobiohydrolase-Ii of trichoderma-Reesei during hydrolysis of microcrystalline cellulose. Biotechnol Bioeng 44(9):1064–1073.

Nakamura A, Watanabe H, Ishida T, Uchihashi T, Wada M, Ando T, Igarashi K, Samejima M. 2014. Trade-off between processivity and hydrolytic velocity of cellobiohydrolases at the surface of crystalline cellulose. J Am Chem Soc 136(12):4584–4592.

Nidetzky B, Hayn M, Macarron R, Steiner W. 1993. Synergism of trichoderma-Reesei cellulases while degrading different celluloses. Biotechnol Lett 15(1):71–76.

Park S, Baker JO, Himmel ME, Parilla PA, Johnson DK. 2010. Cellulose crystallinity index: Measurement techniques and their impact on interpreting cellulase performance. Biotechnol Biofuels 3:10.

Ragauskas AJ, Williams CK, Davison BH, Britovsek G, Cairney J, Eckert CA, Frederick WJ, Hallett JP, Leak DJ, Liotta CL, Mielenz JR, Murphy R, Templer R, Tschaplinski T. 2006. The path forward for biofuels and biomaterials. Science 311(5760):484–489.

Reinikainen T, Henriksson K, Siikaaho M, Teleman O, Poutanen K. 1995. Low-Level endoglucanase contamination in a trichoderma-Reesei cellobiohydrolase-Ii preparation affects its enzymatic-activity on beta-glucan. Enzyme Microb Technol 17(10):888–892.

Singh S, Simmons BA, Vogel KP. 2009. Visualization of biomass solubilization and cellulose regeneration during ionic liquid pretreatment of switchgrass. Biotechnol Bioeng 104(1):68–75.

Sluiter JB, Ruiz RO, Scarlata CJ, Sluiter AD, Templeton DW. 2010. Compositional analysis of lignocellulosic feedstocks. 1. Review and description of methods. J Agric Food Chem 58(16):9043–9053.

Ståhlberg J, Johansson G, Pettersson G. 1991. A new model for enzymatic-Hydrolysis of cellulose based on the 2-Domain structure of cellobiohydrolase-I. Bio-Technology 9(3):286–290.

Ståhlberg J, Johansson G, Pettersson G. 1993. Trichoderma-Reesei has No true exo-Cellulase—All intact and truncated cellulases produce new reducing end groups on cellulose. Biochim Biophys Acta 1157(1):107–113.

Sugimoto N, Igarashi K, Wada M, Samejima M. 2012. Adsorption characteristics of fungal family 1 cellulose-Binding domain from trichoderma reesei cellobiohydrolase I on crystalline cellulose: Negative cooperative adsorption via a steric exclusion effect. Langmuir 28(40):14323–14329.

Van Dyk JS, Pletschke BI. 2012. A review of lignocellulose bioconversion using enzymatic hydrolysis and synergistic cooperation between enzymes-Factors affecting enzymes, conversion and synergy. Biotechnol Adv 30(6):1458–1480.

Wang LS, Zhang YZ, Gao PJ, Shi DX, Liu HW, Gao HJ. 2006. Changes in the structural properties and rate of hydrolysis of cotton fibers during extended enzymatic hydrolysis. Biotechnol Bioeng 93(3):443–456.

Wiley JH, Atalla RH. 1987. Band assignments in the raman-Spectra of celluloses. Carbohydr Res 160:113–129.

Wingren A, Galbe M, Roslander C, Rudolf A, Zacchi G. 2005. Effect of reduction in yeast and enzyme concentrations in a simultaneous-saccharification-and-fermentation-based bioethanol process. Technical and economic evaluation. Appl Biochem Biotechnol 121–124:485–499.

Wooley R, Ruth M, Glassner D, Sheehan J. 1999. Process design and costing of bioethanol technology: A tool for determining the status and direction of research and development. Biotechnol Prog 15(5):797–803.

Wyman CE. 2007. What is (and is not) vital to advancing cellulosic ethanol. Trends Biotechnol 25(4):153–157.

Yang B, Dai Z, Ding S-Y, Wyman CE. 2011. Enzymatic hydrolysis of cellulosic biomass. Biofuels 2(4):421–450.

Yang B, Willies Deidre M, Wyman Charles E. 2006. Changes in the enzymatic hydrolysis rate of Avicel cellulose with conversion. Biotechnol Bioeng 94(6):1122–1128.

Zhang S, Wolfgang DE, Wilson DB. 1999. Substrate heterogeneity causes the nonlinear kinetics of insoluble cellulose hydrolysis. Biotechnol Bioeng 66(1):35–41.

Zhu Z, Sathitsuksanoh N, Percival Zhang YH. 2009. Direct quantitative determination of adsorbed cellulase on lignocellulosic biomass with its application to study cellulase desorption for potential recycling. Analyst 134(11):2267–2272.

Supporting Information

Additional supporting information may be found in the online version of this article at the publisher's web-site.